The rapid formation of macromolecules in irradiated ice of protoplanetary disk dust traps

Ligterink, Niels F.W.; Pinilla, Paola; van der Marel, Nienke; van Scheltinga, Jeroen Terwisscha; Booth, Alice S.; Alexander, Conel M.O.D.; Riebe, My E.I.

DOI
10.1038/s41550-024-02334-4

Publication date
2024

Published in
Nature Astronomy

nature astronomy

Article

https://doi.org/10.1038/s41550-024-02334-4

The rapid formation of macromolecules in irradiated ice of protoplanetary disk dust traps

Received: 19 October 2023

Accepted: 10 July 2024

Published online: 30 July 2024

Check for updates

Niels F. W. Ligterink[1,2] ✉, Paola Pinilla[3], Nienke van der Marel[4], Jeroen Terwisscha van Scheltinga[4,5], Alice S. Booth[4,6], Conel M. O'D. Alexander[7] & My E. I. Riebe[8]

Organic macromolecular matter is the dominant carrier of volatile elements such as carbon, nitrogen and noble gases in chondrites—the rocky building blocks from which Earth formed. How this macromolecular substance formed in space is unclear. Here we show that its formation could be associated with the presence of dust traps, which are prominent mechanisms for forming planetesimals in planet-forming disks. We demonstrate the existence of heavily irradiated zones in dust traps, where small frozen molecules that coat large quantities of microscopic dust grains could be rapidly converted into macromolecular matter by receiving radiation doses of up to several tens of electronvolts per molecule per year. This allows for the transformation of simple molecules into complex macromolecular matter within several decades. Up to roughly 4% of the total disk ice reservoir can be processed this way and subsequently incorporated into the protoplanetary disk midplane where planetesimals form. This finding shows that planetesimal formation and the production of organic macromolecular matter, which provides the essential elemental building blocks for life, might be linked.

Organic macromolecular matter probably supplied the terrestrial planets with most of their carbon, nitrogen and noble gases[1]. In chondrites, this material is often called insoluble organic matter (IOM), where it is the dominant carrier of these volatile elements[2]. It has even been suggested that organic macromolecular matter directly contributed to the emergence of life[3]. Similarities in the elemental compositions of chondritic IOM and refractory organic matter in comets, as well as large deuterium enrichments, indicate that there is a genetic relationship between the two materials[4]. A genetic relationship is, perhaps, not so surprising since the formation regions of some chondrites were probably well beyond the orbit of Jupiter[5]. Hence, refractory organic matter was distributed over large radial distances in the proto-solar nebula[6]. Detailed characterization of IOM has provided constraints for potential formation mechanisms, but there is still no consensus about whether this material formed in the interstellar medium, the proto-solar nebula or planetesimals by polymerization of simpler precursors[2]. With a new model, we demonstrate that macromolecular organic matter resembling that of IOM in chondrites[2] and refractory organics in comets[6] could rapidly form in dust traps in the proto-solar nebula, via radiation-driven ice chemistry. Large quantities of ice, up to roughly

[1]Physics Institute, Space Research and Planetary Sciences, University of Bern, Bern, Switzerland. [2]Faculty of Aerospace Engineering, Delft University of Technology, Delft, The Netherlands. [3]Mullard Space Science Laboratory, University College London, Dorking, UK. [4]Leiden Observatory, Leiden University, Leiden, The Netherlands. [5]Laboratory for Astrophysics, Leiden Observatory, Leiden University, Leiden, The Netherlands. [6]Center for Astrophysics, Harvard and Smithsonian, Cambridge, MA, USA. [7]Earth and Planets Laboratory, Carnegie Institution for Science, Washington, DC, USA. [8]Institute of Geochemistry and Petrology, Eidgenössische Technische Hochschule Zürich, Zurich, Switzerland. ✉e-mail: niels.ligterink@tudelft.nl

4% of the total disk ice reservoir in our model, could be processed in this way and later incorporated into planetesimals. Our findings suggest a link between the mechanism that forms planetesimals and the chemical processes that determined their macromolecular and volatile element budgets.

Due to the steady influx of meteorites to Earth, IOM is the best studied of all extraterrestrial macromolecular organic matter. Its structure is characterized by small (poly)cyclic aromatic units, linked by short, highly branched aliphatic chains, furan/ether bonds and additional functional groups, such as ketones and carboxyls[7,8]. Deuterium and ^{15}N enhancements in bulk, and even larger ones in individual grains, require cold (<20 K) and radiation-rich environments where isotopes are readily fractionated, and simple molecules are frozen onto dust grains[9]. Subsequent radiation of frozen organics could enhance deuterium enrichments[10], while heating and aqueous alteration in the parent bodies may have reduced them[11]. IOM contains radicals in its structure[12,13] that may have been generated during irradiation of organic molecules[14]. IOM also contains high concentrations of noble gases that are isotopically fractionated and depleted in light noble gases compared with the solar composition[15], which is suggestive of a thermal loss mechanism starting at low temperatures (<100 K).

These observations suggest that the formation of IOM and refractory organics in comets involves the irradiation of frozen carbon-bearing molecules. Laboratory studies of particle and ultraviolet (UV) irradiation of ice films and frozen organic molecules have demonstrated that these molecules can be converted into macromolecular matter[16–19], although mixing ratios in the experiments are not always realistic with respect to the ice found in interstellar environments and protoplanetary disks. Radiation doses of several hundred up to a thousand electronvolts per molecule are required for the conversion, which is much higher than what molecules in the solid phase typically experience during the star- and planet-formation cycle. UV and cosmic-ray doses received by ice-coated grains in dark clouds and protoplanetary disk midplanes at most reach several tens of electronvolts per molecule (~10^{-7} eV per molecule per year)[20]. Radiation doses received by ice-coated dust grains in the outer layers of a protoplanetary disk, which are directly irradiated by the protostar, are similarly moderate and only sufficient to produce much smaller and typically solvent-soluble organic molecules (SOM; such as amino acids, sugars, polyoxymethylene and other polymers)[21]. Until now, it was unknown where large quantities of ice and other frozen materials could be heavily irradiated to form organic macromolecular matter during the star- and planet-formation sequence.

Following the first detection of a dust trap in the protoplanetary disk IRS48 (ref. 22), our understanding of planetesimal formation has been revolutionized[23]. Dust traps are localized pressure bumps in protoplanetary disks where the radial drift of dust is reduced or stopped and material piles up[24]. Grains in these traps can efficiently grow to form pebbles and pebbles may be further concentrated by the streaming instability to form planetesimals[23,25]. Dust traps are regularly found in protoplanetary disks with different properties (for example, disk ages from <1 to 10 Myr) and in the form of rings and crescents in millimetre dust continuum observations with the Atacama Large Millimeter Array[23]. They are thought to have played a fundamental role in the formation of the Solar System, as they were probably present in the primordial disk, even beyond the current orbit of Uranus[26]. Based on their distinct isotopic compositions, the different carbonaceous chondrite groups that host IOM have been suggested to have collected in a dust trap that formed in the first 2–4 Myr (ref. 27).

Dust traps have been observationally shown to contain large amounts of ice-associated molecules that were probably inherited from the molecular cloud stage[28]. H_2CO, CH_3OH and CH_3OCH_3 have recently been detected in the gas phase in a region that is co-spatial with dust traps[29–31]. The detection of these molecules can be explained by the vertical transport of ice-coated grains and thermal desorption in the warmer surface layers, whereas in disks without dust traps these molecules remain locked up in ice-coated grains, thus remaining undetectable with the Atacama Large Millimeter Array[32]. Hence, vertical transport of ice to irradiated zones of dust traps potentially provides favourable conditions for the formation of organic macromolecules.

In this study, we use the output of a state-of-the-art dust evolution model of a protoplanetary disk with a dust trap[33] and calculate the UV radiation dose rate in ice-coated grains throughout the disk. While we knew of radiation-heavy and ice-rich interstellar environments, before our work there was no known environment in a planet-forming disk where high radiation doses and large ice reservoirs (on the percent level) coincided, as most of the ice-coated grains were thought to be well shielded from radiation. We demonstrate the existence of heavily irradiated regions in dust traps, where large ice reservoirs can rapidly be transformed into organic macromolecular matter such as IOM.

Results

The dust and gas distributions predicted by the dust evolution model for a 1-Myr-old protoplanetary disk with a dust trap at 45 astronomical units (AU) are shown in Fig. 1a,b (details in Methods). The dust-to-gas ratio exceeds unity in the dust trap of this model, which is a sign that planetesimal formation ensues. The modelled dust grain sizes range from 10^{-7} to 10^{-1} m, but grains smaller than several tens of micrometres dominate at elevated heights in the dust trap (Extended Data Fig. 1). The assumption is made that each dust grain is covered by 100 monolayers (ML; where 1 ML is 10^{15} molecules cm^{-2}) of frozen molecules. Since we determine the average dose rate per molecule, the composition of the ice is arbitrary, but it can be thought to resemble those of interstellar dust grains, that is, H_2O dominated, with fractions of CH_4, CO, CO_2, CH_3OH and NH_3. Alternatively, warm grains can be coated in a layer of non-volatile organic molecules after water ice has sublimated[34]. UV photons emitted by the protostar penetrate throughout the disk (Fig. 1c) and the photon flux is calculated as a vertical radiation field, which is attenuated by the gas and dust throughout the disk. The optical depth is determined following $\tau(R,Z) = \int_Z^\infty \rho(R,Z)\kappa \mathrm{d}Z$, where the column of material at a radius R from the central star above a height Z above the midplane is multiplied by the average opacity κ (cm^2 g^{-1}). The UV flux is calculated with the Beer–Lambert law $F(R,Z) = F_0 \mathrm{e}^{-\tau(R,Z)}$, where F_0 is the number of incoming photons. In the fiducial model, we use $F_0 = 1{,}000G_0$, where G_0 is a UV flux of 10^8 photons cm^{-2} s^{-1}. Various models of protoplanetary disks demonstrate that this is a flux that is readily achieved in the surface layers of disks, due to the radiation from the central star[35]. The mean opacity is set to $\kappa = 10$ cm^2 g^{-1}, which is a value commonly used for protoplanetary disks[36].

The grain photon flux (product of the photon flux and the grain surface areas) of the fiducial model is shown in Fig. 1d,e. It reveals that the largest reservoir of ice-coated dust grains receiving the largest photon flux is in the dust trap at $Z = \pm 10$ AU and $R = 45$ AU. This is the result of local gas densities being lower near the inner edge of the dust ring or dust trap, while dust densities are large. In comparison, gas densities in the inner disk (taken as $r < 10$ AU in our model) are large (Fig. 1b) and only minor quantities of disk ice receive an appreciable photon flux (Fig. 1d). In the dust trap at a height of $Z = 5$–20 AU, grain temperatures generally exceed ~50 K, while submicrometre grain temperatures surpass even ~100 K in specific regions (Fig. 1f and Extended Data Fig. 2). Therefore, most grains in the dust trap are 'luke-warm' and retain ice films that are dominated by less volatile species (for example, H_2O, CH_3OH and polycyclic aromatic hydrocarbons (PAHs)), small amounts of trapped more volatile species and minor quantities of other organic molecules[34]. The combination of high dust concentrations, moderately elevated temperatures and radiation makes the dust trap wall a hotspot for radiation-driven ice chemistry, which stimulates the formation of complex molecules[37].

The dust trap hotspot is divided into regions at intervals of 10^{-3}, 10^{-2} and 10^{-1} times the peak grain flux ($F_{\mathrm{gr,peak}}$). By dividing the incoming

https://doi.org/10.1038/s41550-024-02334-4

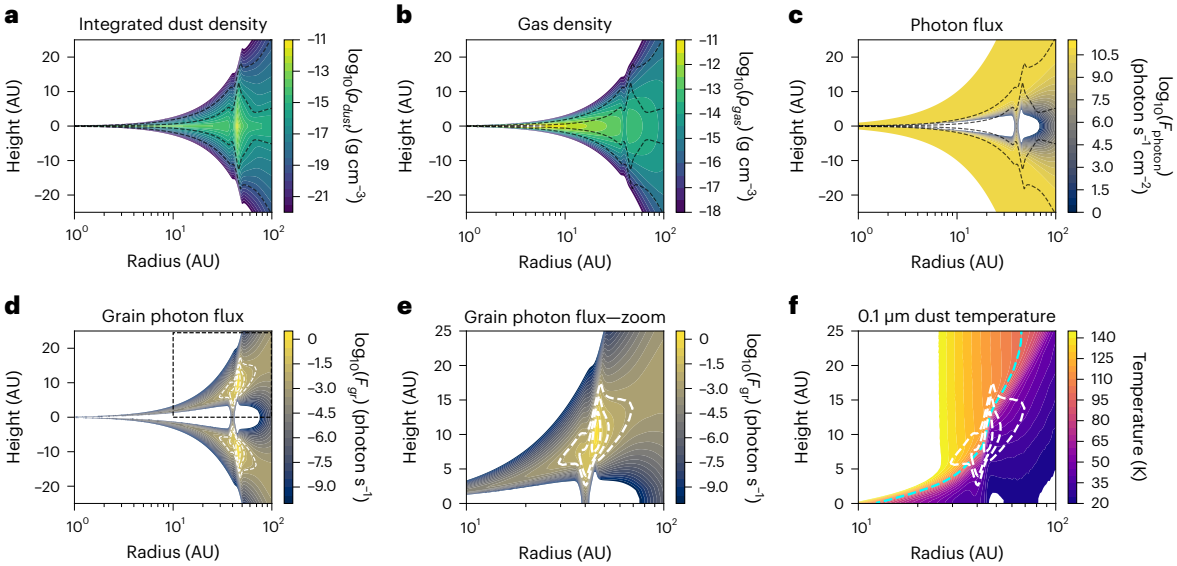

Fig. 1 | Dust evolution and irradiation model of a protoplanetary disk with a dust trap located at ~45 AU. a–**f**, The integrated dust density distribution (**a**), gas density (**b**), photon flux for an opacity of $\kappa = 10\ \mathrm{cm^2\ g^{-1}}$ (**c**), grain photon flux (**d**; close-up in **e**) and temperature of the 0.1 μm dust grains (**f**) are shown. The black contours indicate the dust density at 10^{-19} (outer) and 10^{-16} (inner) g cm^{-3}, the hotspot region is depicted by white contours at 10^{-3}, 10^{-2} and 10^{-1} times the peak grain photon flux, and the cyan contour indicates the boundary where the grain temperature equals 100 K.

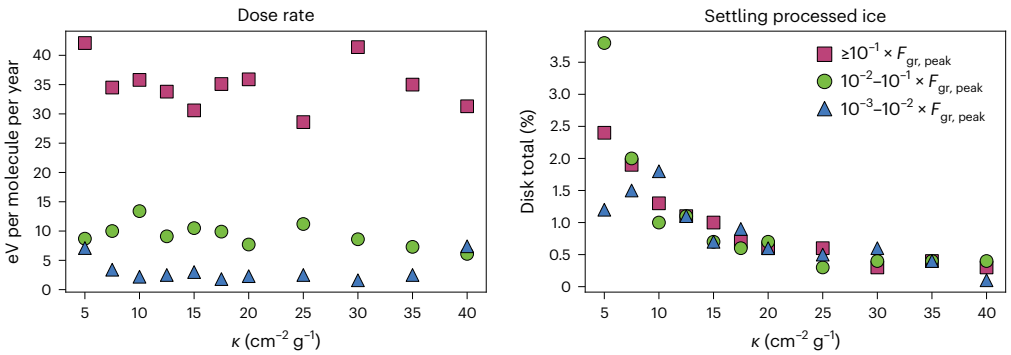

Fig. 2 | Influence of the opacity on the dose rate and amount of settled processed ice for regions constrained between 10^{-3}, 10^{-2} and 10^{-1} times the peak grain photon flux. While the dose rate remains constant, the amount of processed ice that can settle back to the midplane increases with decreasing disk opacity.

photon flux by the amount of ice and assuming an average UV photon energy of 6 eV (ref. 38), the average energetic input is determined in electronvolts per molecule per second for all molecules in the ice mantle, including H_2O. At its peak position, the fiducial model shows that the dose rate is 36 eV per molecule per year. A dose of 1,000 eV per molecule, which is sufficient to produce macromolecular matter[16–18], is achieved within 30 years. Even in the extended region, where the dose rate decreases to 2 eV per molecule per year, this dose is obtained in approximately 500 years. These timescales are well within the expected lifetime of a dust trap[24].

A substantial quantity of ice is contained in the hotspot region, with 2.6%, 2.1% and 3.5% of the total disk ice reservoir in the three regions, respectively (8% total). Grains are subject to vertical turbulence, which results in the loss of ice-coated grains to the disk atmosphere when grains are stirred upwards. For this model, approximately half of the grains are lost (see Methods for details), which means that the other half (4%) of the processed ice reservoir settles to the disk midplane, where it is available as planetesimal-forming material. Because such a large quantity of ice is processed, organic macromolecular matter formation in dust traps can currently best explain the ~6% formation efficiency of IOM and up to 55% for comets as derived from atomic C/Si ratios[2]. The ice-conversion factor is probably higher in a dynamic disk where fresh ice-coated grains are continuously replenished in the dust trap hotspot due to vertical and radial mixing. Conversion efficiencies of pristine ice to organic macromolecular matter have not been determined, and therefore, the amount of processed ice is an upper limit of produced macromolecular matter. Furthermore, dust trap locations and opacities may differ from disk to disk and will critically influence the dose rates and above-derived conversion fraction. For opacities ranging from 5 to 40 $\mathrm{cm^2\ g^{-1}}$, the average dose rate does not alter substantially for this model (Fig. 2, left), but the amount of processed frozen material increases with decreasing κ (Fig. 2, right). This is the result of photons penetrating deeper into the disk, that is, closer to the midplane, and accessing regions where the concentration of dust grains is larger.

Discussion

The following scenario for the formation of macromolecular matter is proposed (Fig. 3). In dense interstellar clouds, dust grains acquire ice mantles of simple species that are enriched in minor isotopes[39,40]. The ice or dust grain may be enriched in PAHs. Heavy noble gases are efficiently trapped in these ice mantles[41], and moderate grain surface chemistry results in the production of minor quantities of SOM[42]. The protoplanetary disk inherits these ice-coated grains from its host

https://doi.org/10.1038/s41550-024-02334-4

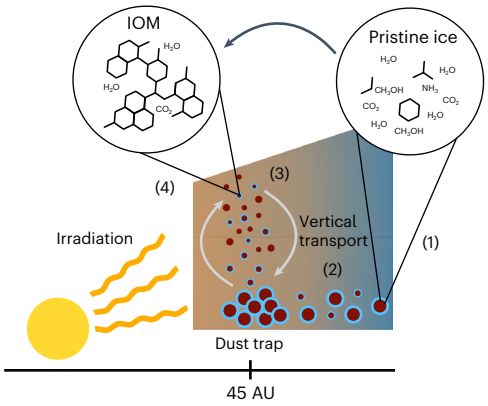

Fig. 3 | Schematic depiction of the IOM formation scenario. Grains with pristine, simple ice components (1) radially drift into the protoplanetary disk (2) and migrate to the dust trap hotspot through vertical mixing/transport (3), where heavy irradiation of the luke-warm ice results in the formation of organic macromolecular matter (4).

cloud[28]. As grains migrate into the dust trap hotspot, the ice warms up and the UV flux increases, resulting in a rapid conversion of the organic material in the ice mantle into macromolecular matter, by producing and linking complex ice-irradiation products, such as low-volatility SOM, and PAH fragments[43–45]. Noble gases in the ice mantles may be trapped in the macromolecular matter during this process[46], and D isotopic signatures could be fractionated during further irradiation due to preferential loss of light isotopes[10,14]. Processed grains are cycled back into the midplane, creating a mixture of pristine ice and macromolecular matter, in line with the fact that chondrites accreted substantial amounts of ice[47]. Migration of these mixtures closer to the protostar can result in IOM-rich objects such as the asteroid Ryugu[48], whereas staying at these large radii (45 AU in this model) preserves it as refractory organics as seen in comets[49]. Since multiple dust traps can occur in a protoplanetary disk, cometary refractory organics and IOM in meteorites and asteroids may be formed at different radii and times. In both cases, the heavy irradiation of grain mantles results in the production of similar macromolecules.

In bulk and at the grain (micrometre to submicrometre) scale, IOM shows a range of chemical and isotopic characteristics[2,50], which can be explained by this scenario. Disks are turbulent environments[24], creating variations in photon flux and grain surface temperature. Protoplanetary disks can have multiple dust traps at different radii with different shapes and amplitudes, and the flux of radiation from the central star can vary with time[23], which would further enhance the diversity of macromolecular products and their characteristics. For example, deuterium fractionation by irradiation of organic polymers has been demonstrated, where different radiation fluxes will result in different levels of fractionation on top of the inherited signature[10]. The mixing of material that experienced different degrees of alteration of these pathways explains the heterogeneous isotope nature of IOM on (sub)micrometre scales[50]. Small (sub)micrometre ice-coated dust grains are preferentially stirred up into the hotspot region (Extended Data Fig. 1), but trajectories and residence times may vary from a few to several dozen Ω_k^{-1} (in this model, Ω_k^{-1} is ~30–50 years at the hotspot radius)[51]. However, because small grains are continuously re-created in the trap owing to the fragmentation of the large particles, there is a continuous population of small grains present for million-year timescales that are exposed to the irradiation needed for IOM formation. This affects the transformation of pristine material into organic macromolecular matter and, in turn, its chemical composition and the texture of the material. For example, nanoglobules, small spherical and often hollow macromolecular grains[52,53], have been suggested to have formed by UV irradiation of ice mantles of (sub)micrometre-sized grains[53], although alternative formation pathways by aqueous alteration have been suggested as well[8].

A prominent question that remains is whether organic macromolecular matter is formed in a water-rich or water-poor environment. Ice mixtures in irradiation experiments that produce IOM analogues contain minor amounts of or no water[17,18] and do not match with the known ice compositions of interstellar ice-coated dust grains or comets[34]. Water-rich ice is expected to lead to enhanced CO_2 formation and oxygen-rich macromolecular material, inconsistent with the carbon-rich elemental composition of organic macromolecular matter observed in meteorites and comets. From the experimental work conducted thus far, it is unknown whether macromolecular matter can form in water-dominated ice. Instead, its formation may rely on a preceding step where low-volatility SOM is formed, water ice is removed (for example, by thermal desorption)[42], and followed by heavy irradiation to form complex refractory macromolecules[16,19]. In our model, some of the smallest dust grains, which dominate the dust composition in the hotspot, reach temperatures at which water ice readily sublimates. If a dust trap is located closer to the protostar, grains of larger sizes will be heated up to higher temperatures and the loss of water ice becomes more prominent, while organics of low volatility remain. A thermal heating cycle may also have further depleted Ar and Kr relative to Xe, resulting in the low Ar/Xe and Kr/Xe ratios in natural IOM.

To determine the required dose to form organic macromolecular matter, we cite particle irradiation studies[16–18], whereas our model relies on UV radiation. Photons are affected by the optical properties of the ice, whereas penetration depths of particles of kiloelectron volts and larger energies are usually larger than UV photons. These differences may result in different chemical outcomes of ice irradiation. However, experimental products are the same for ice films irradiated with UV photon or ions at similar dose[54]. This makes it plausible that both radiation types will result in a similar type of organic macromolecular matter, as indirectly indicated by UV irradiation experiments[19].

In the past few years, high-resolution observations of protoplanetary disks have demonstrated that disks have dust traps irrespective of their properties or those of their central star. We demonstrate that hotspots, that is, zones of heavy irradiation and increased dust temperatures, exist in these dust traps, where the icy mantle material on dust grains can rapidly be converted to organic macromolecular matter. Since dust traps are also likely places for efficient planetesimal formation, this suggests that the mechanism by which planetesimals form also produced the macromolecular matter from which the terrestrial planets derive their elemental carbon and nitrogen, which in the case of the Earth contributed to the emergence of life.

Methods

The dust evolution models are performed using the Dustpy code[55]. The disk is assumed to be around a solar-mass star, with a gas surface density that assumes a critical radius at 80 AU and an initial disk mass of 5% of the Sun[24]. The model assumes a fragmentation velocity of $v_f = 10\ \mathrm{m\ s^{-1}}$, a gas viscous evolution parameter, radial diffusion, turbulent mixing and vertical settling/stirring all set to 10^{-4}. All grains are initially small between 0.1 and 1 μm in size, with a power law distribution as $n(a) \propto a^{-3.5}$. The models include the dust growth and dynamics of particles. The model output gives the density distribution of the dust grains (Fig. 1a, ρ_{dust}) and of the gas (Fig. 1b, ρ_{gas}) at 1 Myr of evolution. The data are portrayed in a radial grid from 1 to 300 AU (only 1 to 100 AU shown in Fig. 1) with 300 logarithmically spaced cells. A logarithmically spaced grain size distribution between the minimum grain size of 0.1 μm to 0.1 m in 127 steps is used. A gap centred at 40 AU is assumed in the disk[33], which yields a pressure bump at around 45 AU. Smaller and lighter dust grains are more easily stirred up in the disk and therefore dominate the particle sizes at greater disk heights, whereas larger particles concentrate around the disk midplane (Extended Data Fig. 1)

From the dust density distribution, the grain surface area is calculated by assuming that all grains are spherical and have a density of $\rho_{grain} = 1.65\ g\ cm^{-3}$. This allows us to calculate the particle mass for each grain size and convert the dust density (g cm^{-3}) into a particle density (n cm^{-3}). Next, the particle density is multiplied by the grain area to find the total grain area per volume, which gives

$$A_{grain} = \frac{(3\rho_{dust})}{(\rho_{grain} r_{grain})}, \quad (1)$$

where r_{grain} is the grain size (that is, the radius). Using the grain area, the available amount of ice is calculated by assuming that each grain is covered with 100 MLs (1 ML is 10^{15} molecules cm^{-2}) of ice and by multiplying this value with the available grain surface area.

The thermal structure of the disk is modelled with RADMC-3D[56], assuming a vertical grid of 180 cells over a semicircle following $Z = R\cos(\theta)$, where Z is the disk height and R the radius, and following the same procedure as ref. 33. The grain sizes that dominate the dust trap hotspot have sizes of 0.1 to several tens of micrometres and generally have temperatures greater than 50 K. However, only submicrometre grains are heated above 100 K, and only in specific regions of the hotspot (Extended Data Fig. 2).

The number of photons throughout the disk is calculated with the Beer–Lambert law (Results). The impinging photon flux is fixed to $F_0 = 1{,}000 G_0$ ($G_0 = 10^8$ photons $cm^{-2}\ s^{-1}$), but we note the (grain) photon flux throughout the disk scales linearly with the value chosen for F_0. Therefore, the dose rate can be scaled in the same way. The number of photons absorbed by the mantle depends on its thickness and the UV photon absorption cross-section. Assuming the mantle consists entirely of water ice, then a film of 100 ML does not fully absorb the received flux[57]. The simplified division of the photon energy input by the column density to yield electronvolts per molecule per second is therefore a rough assumption. However, since the photons that penetrate the ice mantle still hit the underlying grain, we assume that the energy is contributed to the overall system and, therefore, the simplified division holds.

Gravitational attraction causes grains to settle in the disk midplane, while turbulent stirring can move particles towards or away from the midplane. The velocities of these processes can be calculated[58] and, in turn, be used to assess how the dust is vertically distributed.

The equation to determine the velocity with which dust settles to midplane is given as

$$v_{sett} = Z\Omega_k \mathrm{ST}, \quad (2)$$

where Z is the vertical height in metres and Ω_k is the Keplerian frequency

$$\Omega_k = \sqrt{\frac{GM_\odot}{R^3}}, \quad (3)$$

where G is the gravitational constant, $M_\odot$ is the solar mass in kilograms, R is the radius in metres and ST is the Stokes parameter, calculated following

$$\mathrm{ST} = \frac{r_{grain}\rho_{grain}}{\Sigma_g}\frac{\pi}{2}, \quad (4)$$

where Σ_g is the gas surface density.

To calculate the vertical velocity, we assume a balance between settling and vertical turbulence and that the later velocity is as the relative velocities due to turbulence of particles of similar size and use

$$v_{stir} = \sqrt{\frac{3\alpha}{\mathrm{ST} + \mathrm{ST}^{-1}}} c_S, \quad (5)$$

where α is the gas viscous evolution parameter ($\alpha = 10^{-4}$) and c_S is the isothermal sound velocity

$$c_S = \sqrt{\frac{k_B T_{gas}}{\mu_{gas} m_{proton}}}, \quad (6)$$

where T_{gas} is the gas temperature ($T_{gas} = 50$ K, the average dust temperature at the trap location and assuming $T_{gas} = T_{dust}$), μ_{gas} is the mean molecular mass of the gas ($\mu_{gas} = 2$) and m_{proton} is the proton mass in kilograms. Note that, in the disk surface, where our calculations are relevant, the dust densities are dominated by the small grains, so the dust particles have similar Stokes numbers, which endorse the use of equation (5) for the stirring velocities.

For the model results used in this work, $v_{stir} \gg v_{sett}$ for the micrometre-sized particles that reside at a greater height in the dust trap. Therefore, stirring determines which direction the material migrates. Since the vertical motion of particles can point in two directions, namely away from the midplane (up) or towards the midplane (down), we assume that the likelihood of up- or downward motion is equal. This means that 50% of the material in the dust trap hotspot goes to the disk atmosphere and 50% moves towards the midplane. We note that this situation holds for a static snapshot of the disk model, but in a dynamic and evolving environment the loss and settle fractions may be different.

Data availability

The datasets used and generated during this study are available via Zenodo at https://zenodo.org/records/11953364 (ref. 59).

Code availability

The code used for this study is available via Zenodo at https://zenodo.org/records/11953364 (ref. 59).

References

1. Marty, B. The origins and concentrations of water, carbon, nitrogen and noble gases on Earth. *Earth Planet. Sci. Lett.* **313**, 56–66 (2012).
2. Alexander, C. M. O. 'D., Cody, G. D., De Gregorio, B. T., Nittler, L. R. & Stroud, R. M. The nature, origin and modification of insoluble organic matter in chondrites, the major source of Earth's C and N. *Geochemistry* **77**, 227–256 (2017).
3. d'Ischia, M. et al. Insoluble organic matter in chondrites: archetypal melanin-like PAH-based multifunctionality at the origin of life? *Phys. Life Rev.* **37**, 65–93 (2021).
4. Paquette, J. A. et al. D/H in the refractory organics of comet 67P/Churyumov-Gerasimenko measured by Rosetta/COSIMA. *Mon. Not. R. Astron. Soc.* **504**, 4940–4951 (2021).
5. Walsh, K. J., Morbidelli, A., Raymond, S. N., O'Brien, D. P. & Mandell, A. M. A low mass for Mars from Jupiter's early gas-driven migration. *Nature* **475**, 206–209 (2011).
6. Kissel, J. & Krueger, F. R. The organic component in dust from comet Halley as measured by the PUMA mass spectrometer on board Vega 1. *Nature* **326**, 755–760 (1987).
7. Hayatsu, R., Matsuoka, S., Scott, R. G., Studier, M. H. & Anders, E. Origin of organic matter in the early solar system—VII. The organic polymer in carbonaceous chondrites. *Geochim. Cosmochim. Acta* **41**, 1325–1339 (1977).
8. Cody, G. D. et al. Establishing a molecular relationship between chondritic and cometary organic solids. *Proc. Natl Acad. Sci. USA* **108**, 19171–19176 (2011).
9. Robert, F. & Epstein, S. The concentration and isotopic composition of hydrogen, carbon and nitrogen in carbonaceous meteorites. *Geochim. Cosmochim. Acta* **46**, 81–95 (1982).
10. Laurent, B. et al. The deuterium/hydrogen distribution in chondritic organic matter attests to early ionizing irradiation. *Nat. Commun.* **6**, 8567 (2015).

11. Alexander, C. M. O'D., Boss, A. P., Keller, L. P., Nuth, J. A. & Weinberger, A. Astronomical and meteoritic evidence for the nature of interstellar dust and its processing in protoplanetary disks. in *Protostars and Planets V* (eds Reipurth, B., Jewitt, D. & Keil, K.) 801–813 (University of Arizona Press, 2007).
12. Binet, L., Gourier, D., Derenne, S. & Robert, F. Heterogeneous distribution of paramagnetic radicals in insoluble organic matter from the Orgueil and Murchison meteorites. *Geochim. Cosmochim. Acta* **66**, 4177–4186 (2002).
13. Alexander, C. M. O. 'D., Nilges, M. J., Cody, G. D. & Herd, C. D. K. Are radicals responsible for the variable deuterium enrichments in chondritic insoluble organic material? *Geochim. Cosmochim. Acta* https://doi.org/10.1016/j.gca.2021.10.007 (2022).
14. Laurent, B. et al. Isotopic and structural signature of experimentally irradiated organic matter. *Geochim. Cosmochim. Acta* **142**, 522–534 (2014).
15. Ott, U. Planetary and pre-solar noble gases in meteorites. *Geochemistry* **74**, 519–544 (2014).
16. Strazzulla, G. & Baratta, G. A. Carbonaceous material by ion irradiation in space. *Astron. Astrophys.* **266**, 434–438 (1992).
17. Ferini, G., Baratta, G. A. & Palumbo, M. E. A Raman study of ion irradiated icy mixtures. *Astron. Astrophys.* **414**, 757–766 (2004).
18. Palumbo, M. E., Ferini, G. & Baratta, G. A. Infrared and Raman spectroscopies of refractory residues left over after ion irradiation of nitrogen-bearing icy mixtures. *Adv. Space Res.* **33**, 49–56 (2004).
19. Danger, G. et al. The transition from soluble to insoluble organic matter in interstellar ice analogs and meteorites. *Astron. Astrophys.* **667**, A120 (2022).
20. Shen, C. J., Greenberg, J. M., Schutte, W. A. & Van Dishoeck, E. F. Cosmic ray induced explosive chemical desorption in dense clouds. *Astron. Astrophys.* **415**, 203–215 (2004).
21. Ciesla, F. J. & Sandford, S. A. Organic synthesis via irradiation and warming of ice grains in the solar nebula. *Science* **336**, 452–454 (2012).
22. van der Marel, N. et al. A major asymmetric dust trap in a transition disk. *Science* **340**, 1199–1202 (2013).
23. Andrews, S. M. Observations of protoplanetary disk structures. *Annu. Rev. Astron. Astrophys.* **58**, 483–528 (2020).
24. Pinilla, P. et al. Trapping dust particles in the outer regions of protoplanetary disks. *Astron. Astrophys.* **538**, A114 (2012).
25. Youdin, A. N. & Goodman, J. Streaming instabilities in protoplanetary disks. *Astrophys. J.* **620**, 459 (2005).
26. Izidoro, A. et al. Planetesimal rings as the cause of the Solar System's planetary architecture. *Nat. Astron.* **6**, 357–366 (2022).
27. Hellmann, J. L. et al. Origin of isotopic diversity among carbonaceous chondrites. *Astrophys. J. Lett.* **946**, L34 (2023).
28. Booth, A. S. et al. An inherited complex organic molecule reservoir in a warm planet-hosting disk. *Nat. Astron.* **5**, 684–690 (2021).
29. van Der Marel, N., Booth, A. S., Leemker, M., van Dishoeck, E. F. & Ohashi, S. A major asymmetric ice trap in a planet-forming disk-I. Formaldehyde and methanol. *Astron. Astrophys.* **651**, L5 (2021).
30. Brunken, N. G. C. et al. A major asymmetric ice trap in a planet-forming disk-III. First detection of dimethyl ether. *Astron. Astrophys.* **659**, A29 (2022).
31. Booth, A. S. et al. Sulphur monoxide emission tracing an embedded planet in the HD 100546 protoplanetary disk. *Astron. Astrophys.* **669**, A53 (2023).
32. van der Marel, N. Transition disks: the observational revolution from SEDs to imaging. *Eur. Phys. J. Plus* **138**, 225 (2023).
33. Pinilla, P., Lenz, C. T. & Stammler, S. M. Growing and trapping pebbles with fragile collisions of particles in protoplanetary disks. *Astron. Astrophys.* **645**, A70 (2021).
34. Boogert, A. C. A., Gerakines, P. A. & Whittet, D. C. B. Observations of the icy universe. *Annu. Rev. Astron. Astrophys.* **53**, 541–581 (2015).
35. Bruderer, S. Survival of molecular gas in cavities of transition disks-I. CO. *Astron. Astrophys.* **559**, A46 (2013).
36. Cevallos Soto, A., Tan, J. C., Hu, X., Hsu, C.-J. & Walsh, C. Inside-out planet formation–VII. Astrochemical models of protoplanetary discs and implications for planetary compositions. *Mon. Not. R. Astron. Soc.* **517**, 2285–2308 (2022).
37. Potapov, A., Fulvio, D., Krasnokutski, S., Jäger, C. & Henning, T. Formation of complex organic and prebiotic molecules in H_2O:NH_3:CO_2 ices at temperatures relevant to hot cores, protostellar envelopes, and planet-forming disks. *J. Phys. Chem. A* **126**, 1627–1639 (2022).
38. Ligterink, N. F. W. et al. Controlling the emission profile of an H_2 discharge lamp to simulate interstellar radiation fields. *Astron. Astrophys.* **584**, A56 (2015).
39. Bacmann, A. et al. CO depletion and deuterium fractionation in prestellar cores. *Astrophys. J.* **585**, L55 (2003).
40. Spezzano, S., Caselli, P., Sipilä, O. & Bizzocchi, L. Nitrogen fractionation towards a pre-stellar core traces isotope-selective photodissociation. *Astron. Astrophys.* **664**, L2 (2022).
41. Almayrac, M. G. et al. The EXCITING experiment exploring the behavior of nitrogen and noble gases in interstellar ice analogs. *Planet. Sci. J.* **3**, 252 (2022).
42. Sandford, S. A., Nuevo, M., Bera, P. P. & Lee, T. J. Prebiotic astrochemistry and the formation of molecules of astrobiological interest in interstellar clouds and protostellar disks. *Chem. Rev.* **120**, 4616–4659 (2020).
43. Qasim, D. et al. Alcohols on the rocks: solid-state formation in a H_3CC CH + OH cocktail under dark cloud conditions. *ACS Earth Space Chem.* **3**, 986–999 (2019).
44. Raut, U., Fulvio, D., Loeffler, M. J. & Baragiola, R. A. Radiation synthesis of carbon dioxide in ice-coated carbon: implications for interstellar grains and icy moons. *Astrophys. J.* **752**, 159 (2012).
45. Qasim, D. et al. Meteorite parent body aqueous alteration simulations of interstellar residue analogs. *ACS Earth Space Chem.* **7**, 156–167 (2023).
46. Sandford, S. A., Bernstein, M. P. & Swindle, T. D. The trapping of noble gases by the irradiation and warming of interstellar ice analogs. *Meteorit. Planet. Sci.* **33**, A135 (1998).
47. Sridhar, S., Bryson, J. F. J., King, A. J. & Harrison, R. J. Constraints on the ice composition of carbonaceous chondrites from their magnetic mineralogy. *Earth Planet. Sci. Lett.* **576**, 117243 (2021).
48. Yabuta, H. et al. Macromolecular organic matter in samples of the asteroid (162173) Ryugu. *Science* **379**, eabn9057 (2023).
49. Blum, J., Bischoff, D. & Gundlach, B. Formation of comets. *Universe* **8**, 381–415 (2022).
50. Busemann, H. et al. Interstellar chemistry recorded in organic matter from primitive meteorites. *Science* **312**, 727–730 (2006).
51. Binkert, F. & Birnstiel, T. Carbon depletion in the early Solar System. *Mon. Not. R. Astron. Soc.* **520**, 2055–2080 (2023).
52. De Gregorio, B. T. et al. Isotopic and chemical variation of organic nanoglobules in primitive meteorites. *Meteorit. Planet. Sci.* **48**, 904–928 (2013).
53. Nakamura-Messenger, K., Messenger, S., Keller, L. P., Clemett, S. J. & Zolensky, M. E. Organic globules in the Tagish Lake meteorite: remnants of the protosolar disk. *Science* **314**, 1439–1442 (2006).
54. Muñoz-Caro, G. M. et al. Comparison of UV and high-energy ion irradiation of methanol: ammonia ice. *Astron. Astrophys.* **566**, A93 (2014).
55. Stammler, S. M. & Birnstiel, T. DustPy: a Python package for dust evolution in protoplanetary disks. *Astrophys. J.* **935**, 35 (2022).
56. Dullemond, C. P. et al. RADMC-3D: a multi-purpose radiative transfer tool. *Astrophysics Source Code Library* http://ascl.net/1202.015 (2012).

57. Cruz-Diaz, G. A., Muñoz-Caro, G. M., Chen, Y.-J. & Yih, T.-S. Vacuum-UV spectroscopy of interstellar ice analogs-I. Absorption cross-sections of polar-ice molecules. *Astron. Astrophys.* **562**, A119 (2014).
58. Birnstiel, T., Fang, M. & Johansen, A. Dust evolution and the formation of planetesimals. *Space Sci. Rev.* **205**, 41–75 (2016).
59. Ligterink, N. Dust_trap_radiation_model. *Zenodo* https://zenodo.org/records/11953364 (2024).

Acknowledgements

We thank E. G. Bøgelund and M. N. Drozdovskaya for insightful discussions. N.F.W.L. is supported by the Swiss National Science Foundation (SNSF) Ambizione Grant 193453. P.P. acknowledges the support from the UK Research and Innovation (UKRI) under the UK government's Horizon Europe funding guarantee from ERC (under grant agreement no. 101076489). A.S.B. is supported by a Clay Postdoctoral Fellowship from the Smithsonian Astrophysical Observatory. M.E.I.R. is supported by the SNSF Ambizione Grant 193331.

Author contributions

N.F.W.L. developed the model with support from P.P. Analysis and interpretation of the model results were performed by N.F.W.L., P.P., N.v.d.M., J.T.v.S., A.S.B., C.M.O'D.A. and M.E.I.R. All authors contributed to writing and review of the paper.

Competing interests

The authors declare no competing interests.

Additional information

Extended data is available for this paper at https://doi.org/10.1038/s41550-024-02334-4.

Correspondence and requests for materials should be addressed to Niels F. W. Ligterink.

Peer review information *Nature Astronomy* thanks Martin Cordiner, Joanna Drążkowska and the other, anonymous, reviewer(s) for their contribution to the peer review of this work.

https://doi.org/10.1038/s41550-024-02334-4

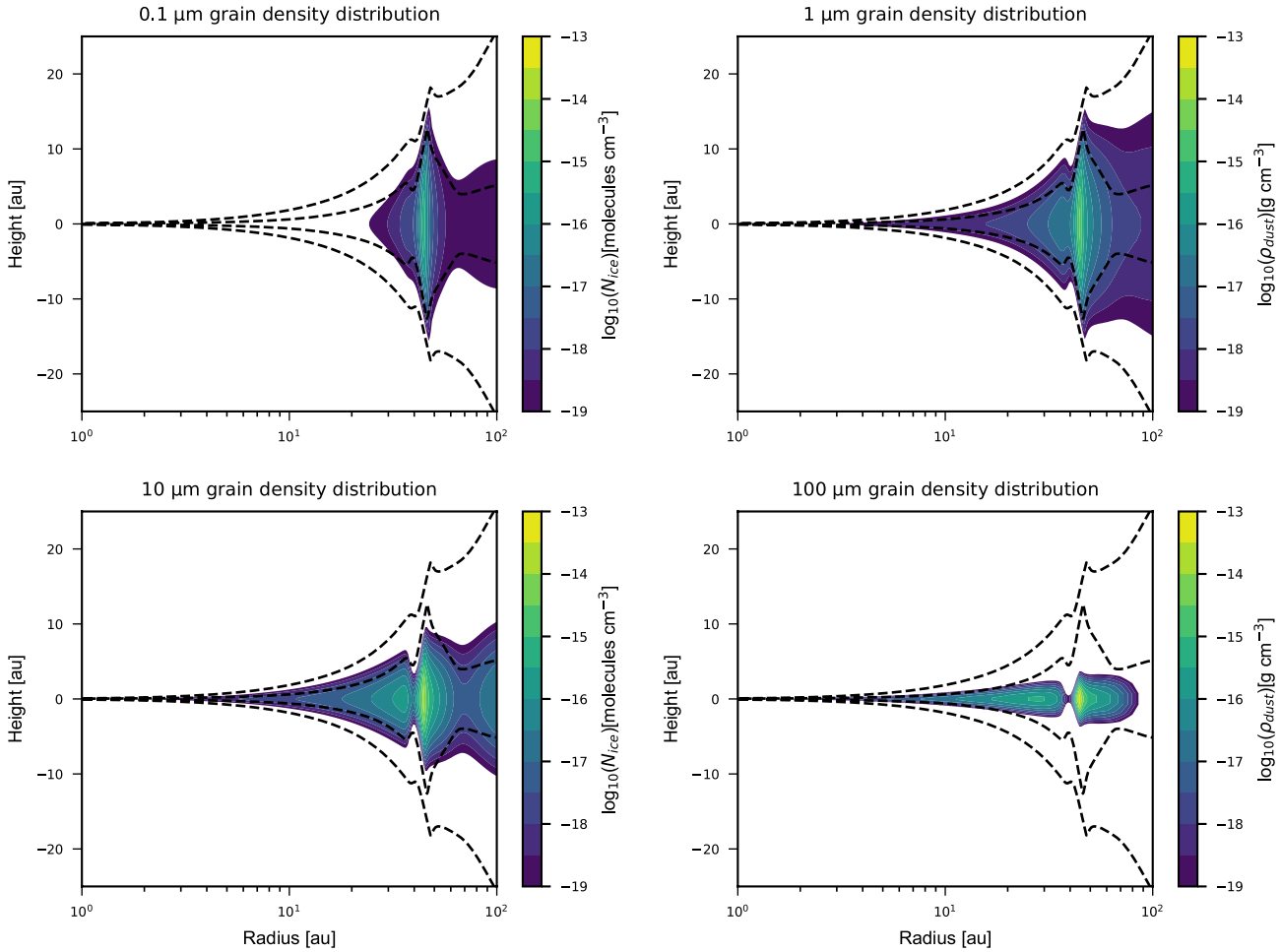

Extended Data Fig. 1 | Dust density distribution for grains of 0.1, 1, 10, and 100 μm in size. The black dashed lines indicate the total dust density distribution contours at 10^{-19} and 10^{-16} g cm^{-3}.

https://doi.org/10.1038/s41550-024-02334-4

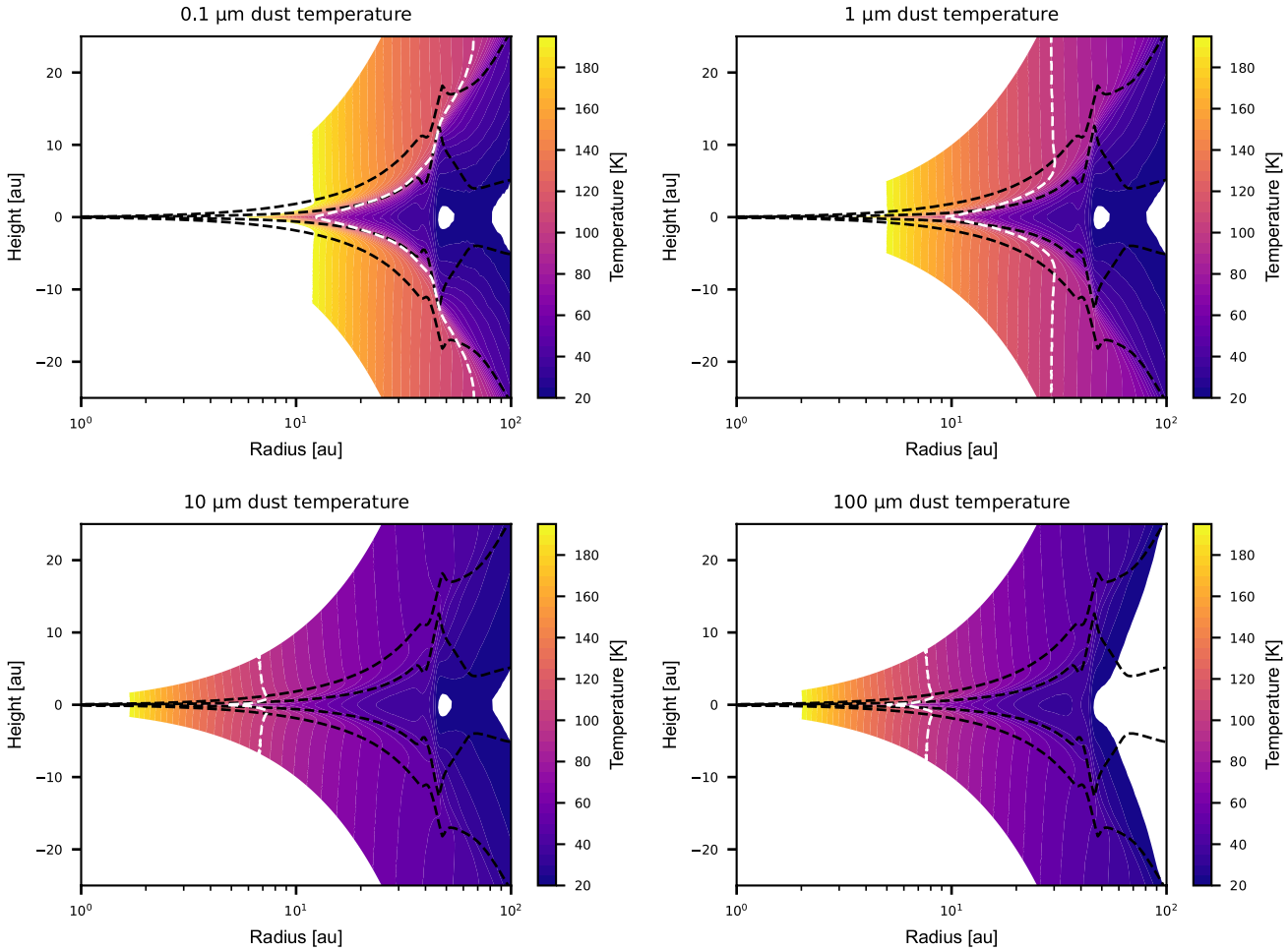

Extended Data Fig. 2 | Dust temperatures for grains of 0.1, 1, 10, and 100 μm in size. The white dashed lines indicate the 100 K temperature contour, while the black dashed lines indicate the total dust density distribution contours at 10^{-19} and 10^{-16} g cm^{-3}.